Stefan M. Holzer[1]

Numerical arch and vault analysis

Analiza numeryczna łuków i sklepień

1. INTRODUCTION

1.1. Continuum-mechanics based approaches

The oldest continuum-mechanics based approach to the numerical analysis of cracking masonry arches is due to Castigliano, 1879 [1, p. 472–478]. Castigliano analyzed the structural behaviour of Ponte Mosca, Turin (erected in 1834). He started with the assumption of a homogeneous, isotropic, elastic arch. After completing the analysis, Castigliano checked, for all radial joints, whether the joints were fully under compression or not. He assumed that the lack of tensile resistance of the mortared (or dry) joints dominates the behaviour of the masonry arch, so that the effective thickness of the arch is reduced to the height of the compressive zone (Fig. 1). In order to capture the mechanics of the arch correctly, it is therefore necessary to perform an iterative analysis. Due to the lack of tensile resistance, the centerline and the thickness of the arch change; the analysis is therefore repeated with the updated geometry, until the change to the preceding iteration is negligible. Castigliano claimed – correctly – that this iterative procedure would converge rapidly. Castigliano's method has found applications until very recently [2]. Castigliano's approach captures the arch mechanics in service state relatively well: The most essential characteristics of masonry, namely the anisotropy related to joint orientation, and the zero tensile strength in the direction normal to the bed joints, are represented in Castigliano's model. The main argument that can be brought forward against Castigliano's model is that it is unsuited for the analysis of the ultimate limit state: It does not permit to introduce the compressive strength of masonry. The compressed part of the arch always remains linear elastic.

More recently, Castigliano's approach has been generalized into multidimensions as the "NTR" material model for arbitrary masonry structures ("non tensile-resistant"; see [3] for a general review and, among other contributions, [4], for specific applications to arches). This approach has been developed aiming at rigourous proofs that material models with zero tensile strength share most of the properties with more classical elastoplastic material laws (based on convex yield surfaces), and that the classical limit theorems of plasticity indeed carry over to such materials. The NTR model can be combined with any isotropic or anisotropic elastic model for the uncracked continuum. It is able to reflect the low tensile strength of masonry without any need of determining a large number of material properties. However, the main drawback of these models is that they do not take into account the orientation-dependent tensile strength of real masonry, but rather assume that masonry has no tensile strength in any direction whatsoever. While this drawback may not be so important within the scope of the analysis of masonry walls where multi-axial in-plane stress and shear dominate, it is a prohibitive drawback when one ventures to analyze vaults, because out-of-plane bending is the most important stress state for vaults.
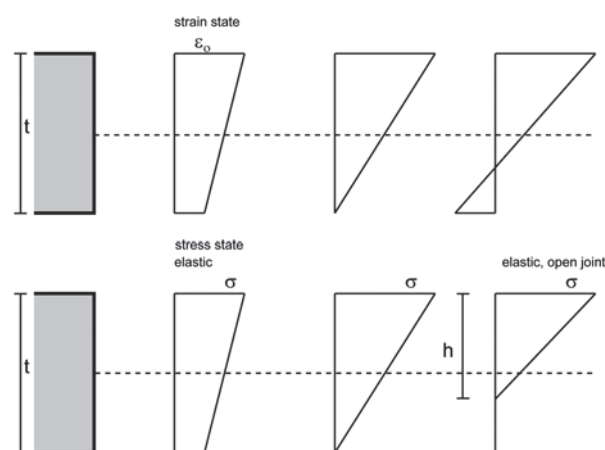

Fig. 1. The one-dimensional NTR (non tensile-resistant) model as implemented by Castigliano

[1] Univ.-Prof. Dr.-Ing. Stefan M. Holzer, Institut BAU-1 (Mathematik & Bauinformatik), Universität der Bundes-wehr München, D-85577 Neubiberg, Germany, stefan.holzer@unibw.de

Conversely, classical plasticity models have also been employed in arch and vault analysis. While some older – in some cases valuable – contributions ([5], [6], [7], [8]) employed isotropic yield surfaces with small tensile strength, more recent contributions have followed the pioneering work of Lourenço for masonry walls (1996, [9]) in employing anisotropic failure criteria ([10], [11]) and have applied them to vaults as well. These models ensure that the vault does not prematurely crack in circumferential direction, an effect which essentially invalidated the analyses of [7], and others, and which commonly occurs when material models for concrete are carried over to the analysis of masonry vaults. Typical historical vault constructions have only one single voussoir stone in thickness direction. In such vaults, cracks follow the radial joint orientation. Circumferential cracks occur only when the tensile stiffness of the stone material is reached, which entails at the same time also the failure of the mortar in the bed joints because the cracking stone is unable to sustain the three-dimensional compressive stress state in the mortar layer. This means, as a consequence, that isotropic elastoplastic material models such as concrete models do not reflect the mechanics of historic thin vaults correctly. Anisotropic elastoplastic models, on the other hand, suffer from the fact that they cannot represent localization of strain: In other words, elastoplastic continuum models must be enriched by discontinuity models in order to capture the development of large, local cracks. Otherwise, they cannot approach the failure state of the vaults, no matter how elaborate the material model or how non-linear the geometric relations used. Furthermore, elaborate anisotropic material models require a large set of input data which are generally extremely difficult to obtain for historic vaults.

The fact that the discrete, localized opening of the radial bed joints of a vault dominates the behaviour of real vaults has been highlighted by [12, p. 104–107]. This model, employing finite elements with discrete unilateral interface elements, but a simple linear elastic model for the voussoir stones, was able to produce results which captured the main effects of the vault behaviour. A similar, but more elaborate, approach has been presented more recently by [13]. This approach employs frictional interface elements. In the paper, the authors have also highlighted that the resulting model shows nonsmooth behaviour and therefore
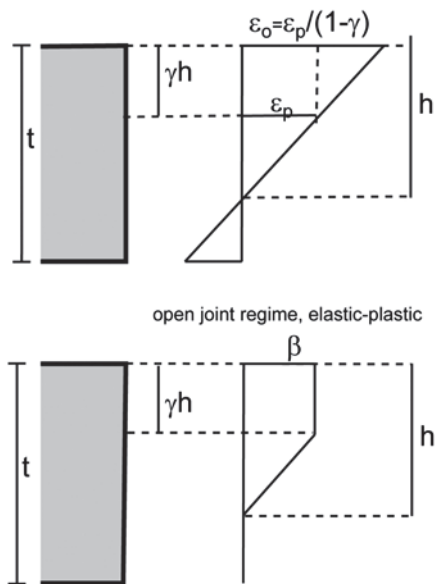
necessitates the use of advanced solvers for the path-following problem. The two studies can be viewed as a transition from the continuum model to the discontinuum models. They capture the role of the joint very well and are able to reproduce the real behaviour of historic arches. The main drawback is that they are based on an individual discretization of the voussoirs and joints and that they require two-dimensional elements for the essentially one-dimensional (curved rod) arch structure. Also, the interface elements must be carried on from the very beginning for all joints of the arch, no matter whether they acquire any importance in the actual course of the loading process. Typically, only a fraction of the joints actually open up, and only few joints reach the compressive limit.

As early as 1985, Crisfield [14] has suggested an arch model based on rod elements and "automatic" introduction of cracking. This was achieved by a numerical integration through the thickness of the arch, taking into account a simple one-dimensional elastic-plastic material law in the direction parallel to the axis of the beam (see also Fig. 2). Crisfield's method "smears" the cracking effects over the element length numerically; however, this means that no discrete, localized interfaces (hinges) develop, so that the deformed figure of the arch is always a smooth curve. In reality, hinges form and the deflection curve exhibits kinks, which cannot be reproduced by smooth finite element ansatz functions. In Crisfield's numerical examples this decisive drawback was not entirely obvious because the arches studied were all shallow arches under considerable backfill. Such arches, which are characterized by high normal stresses, show a tendency towards the formation of extended "plastic zones" instead of localized hinges. This can also be seen in recent contributions which are based on analytical solutions, e.g. [15]: The authors have analyzed an arch under very high backfill (presumed to be an acceptable model for arched openings in walls). Their model is a simple one-dimensional elastic – perfectly plastic model based on Euler-Bernoulli beam kinematics. This model, while perfectly capturing the essentials of arch mechanics, is limited in scope because only simple cases can be solved analytically. When transferred to approximate finite element analysis, it is difficult to reproduce the localizations in the deflections satisfactorily because a smooth finite element function is ill adapted to approximating a curve which exhibits sharp local changes in deflection, up to "kinks". Employing low-order elements, the ultimate load-carrying capacity will be over-estimated because the smooth ansatz functions prevent the formation of hinges; conversely, high-order finite element ansatz functions will lead to oscillations and a break-down of the algorithm far before the true limit load has been reached. The localization problem of arch mechanics – the formation of hinges – within the general scope of an analysis with beam elements has been addressed in 1998 by Molins and Roca [Molins/Roca 1998] by a regularization based on the generation of the beam stiffness matrices by the transfer matrix method; each beam element is discretized into a number of sub-sections; the forward integration in the transfer matrix method permits arbitrary local curvature inside the beam element. The study included a one-dimensional elastic – perfectly plastic material model. The only objection which can be made against this approach is that it requires a complex overall load-stepping procedure, including the storage of path information in all the interior points of the elements and is computationally burdensome because of the necessary sub-element-scale iterations.

Fig. 2 A simple one-dimensional elastic-plastic "opening joint" model

1.2. Rigid-body approaches

The complementary method to elastic, continuum-based analysis is discontinuum analysis, i.e. modeling the vault or arch as an assembly of rigid or elastic/plastic blocks with interfacial contact conditions. In the simplest case, discontinuum analysis boils down to mechanism analysis. The earliest successful attempts at mechanism analysis can be traced back far into history. The first coherent and correct solution was given in the well-known paper of Coulomb of 1773. It was Jacques Heyman's lasting contribution to bring these methods back to practice and to provide them with a modern framework by interpreting them as an application of the limit theorems of plasticity [17]. However, it can be objected against Heyman's original method that the masonry is assumed to be infinitely strong in compression, which is obviously far from true if one considers, e.g., brick vaults with thick mortar joints, a situation frequently encountered in actual historic vaults (typical compressive strength in the order of 1–2 MN/m²). A simple one-dimensional closed-form stress-strain law for masonry with cracking has been presented by [18]. This model includes as a limiting case the linear elastic – perfectly plastic model, although the authors stress the fact that masonry shows a distinct falling branch in the stress-strain curve after the peak. For an extensive review of experimental data, see also [19]. Under the assumption that the elastic – perfectly plastic assumption is nevertheless good enough for all practical purposes, the objection against Heyman's method was successfully tackled by Harvey and others [20] who extended Heyman's "thrust line method" to a method employing a "thrust zone", i.e., a thrust line which is contained within a layer of finite width, corresponding to the compressive strength of the compound material. Harvey's extension to Heyman's method also removed the need to introduce a "geometric factor of safety", which was required in Heyman's original approach because otherwise the stability of an arch under its own weight depends only on the form of the arch, but not on its absolute size (a natural consequence of the infinite strength assumption). Computationally, the Heyman-Harvey method is extremely efficient since it only requires a simple optimization algorithm to identify the critical hinge positions; this optimization can be performed on the basis of an arch which already exhibits three hinges, i.e., it requires only statically determined computations and therefore obviates the need for any material data except the compressive strength. The main objection against the simple hinge mechanism approaches is that they render only an estimate of the limit load, but no information on the sequence of the crack/hinge formation and on the overall load-displacement behaviour. The second objection that they do not include sliding mechanisms is less important. More recently, it has been shown by Ochsendorf [21] and, independently, by Jagfeld [10], that the hinge mechanism (Heyman's or Harvey's approach) approach can be easily extended to geometrically non-linear analyses; in particular, this permits reliable simulations of the problem of the arch on spreading supports, one of the most important questions in the context of assessment of real-life historic arches. In the case of spreading supports, the actual arch transforms quickly into a three-hinged system, so that the hinge mechanism method renders a sharp estimate of the actual behaviour, including the load-displacement behaviour for the arch beyond the point of the formation of the three hinges.

Sliding mechanisms and combinations of hinge and sliding failure are naturally present in more general limit analysis approaches based on rigid or elastic bodies in contact with friction (the reader is referred to [22], [23], [24], [25], [26] for a review). Some of the approaches start from the static limit theorem, others from the kinematic theorem, and they render lower or upper bounds to the true collapse load, respectively. These models require an overall optimization algorithm to identify the failure mechanism. More recently, they have been successfully extended to handle complex cases such as domes, torsional action (see, e.g., [27], [28] and [29]). The most important drawback of all these approaches is that they require block-by-block modelling of the arch masonry and therefore create a great input overhead. Also, these approaches get computationally expensive if a large number of blocks are used, particularly when using elastic blocks and/or complicated constitutive laws for the interfaces. In the analysis of plane arches, sliding occurs only for very shallow geometries (e.g., the platband), or in the case of high horizontal loads, which occur naturally under seismic loading. In the assessment of typical vaults in historic buildings under static loads, sliding is typically not a major concern.

2. A SIMPLIFIED FINITE ELEMENT APPROACH

In the following, we are going to develop a simplified approach for the practical analysis of masonry arches and systems of masonry piers and arches. It is based on the following ideas:

– beam (rod) elements are used
– the strength anisotropy caused by the bed joint orientation is incorporated into the model
– Timoshenko (shear-deformable) theory is employed, allowing the use of low shear stiffnesses for the joints
– the model handles the non-linearity caused by the opening of the joints under flexural stress
– the model is able to detect the formation of plastic hinges and incorporates discrete hinges
– the model incorporates the effect of limited compressive strength
– the model permits accuracy control by *p*-extension (arbitrary polynomial degree of the finite element ansatz functions).

The last item in the list perhaps deserves some explanation. Typically, finite element programs for frameworks use the Euler-Bernoulli beam theory and analytical elemental matrices. This method does no longer work for non-linear stress-strain relationships (However, for an attempt to adapt a commerical finite element code to Castigliano-like analysis, but with limited compressive strength of the material, see [30]). Rather than employing the transfer matrix method for the numerical integration of the element matrices as in [16], we represent the deformation in each beam (displacements in horizontal and vertical direction, rotations) by suitable high-order polynomial approximations (see [31] for an outline of higher-order finite elements). This means that we not only have to handle unknowns at the nodes where the elements are joined, but also inside the individual elements. This approach is natural with Timoshenko beam theory, and it is easily extensible to any non-linear material law. All our computations are achieved with *fixed* meshes; however, the polynomial degree of the *ansatz* functions inside all elements can be varied arbi-

trary. p is increased until it is found that any further increase in the p level has no recognizable effect on the results. Using high p values implies the use of high-degree Gauss-Legendre quadrature schemes for the integration of the element stiffness matrices in axial direction. All the constitutive equations are evaluated at integration point level. The through-the-thickness integration, however, is performed analytically, as opposed to Crisfield's approach [14]. This implies the use of analytical stress-strain laws as explained in the present section.

We start from continuum mechanics assumptions in the serviceability state: Initially, the voussoirs and the mortar are assumed to be linear elastic. Consider an arch of unit width. For given normal force N, there is a certain bending moment M which leads to opening joints. Let $e = \dfrac{M}{N}$ be the associated excentricity of the resultant of the pressures normal to the bed joints (assumed to be orthogonal to the centerline of the arch). Let t denote the thickness of the arch (cf. Fig. 1). Then, at $M_0 = \dfrac{Nt}{6}$, the joint begins to open. We denote by $h \leq t$ the height of the remaining compressive zone. Admitting infinite compressive stress, the maximum bending moment that can be carried by the arch for any given N is $M = \dfrac{Nt}{2}$. For any excentricities $\dfrac{t}{6} < e < \dfrac{t}{2}$, the arch is in the „open joint" regime (Fig. 1). In the open joint regime, the arch with plane sections and linear elastic material carries the bending moment $M = N \cdot \left(\dfrac{t}{2} - \dfrac{h}{3} \right)$. The compressive stress at the compressed edge of the arch is then given by $\sigma = \dfrac{2N}{h}$. Let E denote some average Young's modulus for the masonry under compression. Then, the compressive strain at the compressed edge is $\varepsilon = \dfrac{2N}{Eh}$ and the corresponding curvature of the beam is $\kappa = \dfrac{\varepsilon}{h} = \dfrac{2N}{Eh^2}$. We denote by $\kappa_0 = \dfrac{2N}{Et^2}$ the curvature corresponding to the incipient opening of the joint. Then, $\dfrac{\kappa}{\kappa_0} = \dfrac{t^2}{h^2}$. This way, we obtain the dimensionless relation between bending moment and curvature as

$$\frac{M}{M_0} = 3 - \frac{2}{\sqrt{\kappa / \kappa_0}}.$$

While the joints are completely under compression, purely (linear) elastic deformation dominates. Once the joints start to open, the non-linearity caused by the opening joints becomes the most important feature. The joints are discrete gaps. Nevertheless, the effect of elastically opening joints can be smeared by simple volume averaging. Let α be the volume fraction of the mortared joints (thickness fraction of bed joints in direction parallel to the axis of the arch) and $1 - \alpha$ the volume fraction of the voussoir stones (in historic brick 5% $\leq \alpha \leq$ 25% vaults, typically). Then, considering the joints and the stones as

a serial arrangement of springs, we obtain the averaged normal stiffness of the uncracked arch approximately as

$$(Et)_{arch} = \frac{1}{\dfrac{1-\alpha}{(Et)_{stone}} + \dfrac{\alpha}{(Eh)_{mortar}}}.$$

This relation (and similar ones for the bending and shear stiffnesses) can be readily implemented in a finite beam element. This is essentially Castigliano's approach (except that Castigliano used $(Eh)_{stone}$ instead of $(Et)_{stone}$, an assumption which is retrieved here if we set $\alpha = 1$). This model is perfect for analysing a clamped masonry arch on rigid supports under its own weight. However, any local bending perturbation introduced by local loads on top of the arch will quickly lead to local crushing of the masonry, i.e., to the incipient formation of hinges. The same holds true for yielding supports and the resulting movement. Therefore, the model has to be extended to incorporate the crushing strength β of the masonry. The simplest possible model is the linear elastic – perfectly plastic model (bilinear stress-strain relationship for compression normal to the bed joint). In elastoplastic state (cf. Fig. 2), the compressive zone of height h carries the normal force $N = h\beta \dfrac{1+\gamma}{2}$, where γh is the portion of the compressive zone in which the compressive stress has already reached the limit value β (plastic part of the section). The bending moment which can be carried under these cirumstances can be readily computed to be $M = \dfrac{h\beta}{2} \left(\dfrac{t}{2}(1+\gamma) - \dfrac{h}{3}(1+\gamma+\gamma^2) \right)$. In order to obtain a dimensionless relation between bending moments and curvature again, we introduce the normal capacity $N_p = \beta t$ of the section under uniform pressure and the (arbitrary) reference bending moment $M_p = \dfrac{\beta t^2}{12}$. Now, we can write the dimensionless stress resultants $n = \dfrac{N}{N_p}$ and $m = \dfrac{M}{M_p}$, and we obtain the dimensionless interaction law for combined normal and bending loads:

$$m = 6n - 8\frac{1 + \dfrac{\gamma^2}{1+\gamma}}{1+\gamma} n^2.$$

This formula describes, in the dimensionless interaction diagram, the permissible stress states of the arch under combined axial and bending action. For $\gamma = 0$, we obtain a perfectly "brittle" material model, whereas $\gamma = 1$ would correspond to an infinitely ductile material, permitting arbitrarily large rotations in the plastic regime. Concrete is able to accomodate "ductile" deformation up to $\gamma \approx 0.81$.

While the dimensionless interaction diagram has already been studied by many people and has been made the starting-point of analytical solutions (e.g., [15]), the model proposed so far is unfortunately not very suitable for incorporation into a finite element programm. The reasons for this perhaps somewhat surprising statement become evident if we use the model to derive the associated moment-curvature relation for fixed axial force. Typical historical vaults are in the range of

$n \leq 0.25$. For $n \leq 0.5$, in the elastic – perfect plastic model, the dimensi0onless curvature of the beam is given by

$$\frac{\kappa}{\kappa_0} = \frac{1}{4n^2}\frac{1+\gamma}{1-\gamma}.$$

This relation can be used to eliminate the variable γ describing the extent of plastification inside the compressive zone, yielding

$$\gamma = \frac{\dfrac{\kappa}{\kappa_0} - \dfrac{1}{4n^2}}{\dfrac{\kappa}{\kappa_0} + \dfrac{1}{4n^2}}.$$

If this expression is inserted into the expression for the interaction between moment and axial action, we obtain, in a straighforward way, for any fixed n, a dimensionless moment-curvature relation, $m = m\left(n, \dfrac{\kappa}{\kappa_0}\right)$. Fig. 3 shows this moment-curvature relation for a fixed non-dimensional axial action $n = 0.2$. For comparison, the purely elastic "Castigliano" relationship is also shown. It is evident that the introduction of a finite compressive strength transforms the monotonically growing moment of Castigliano's model into an almost horizontal branch.
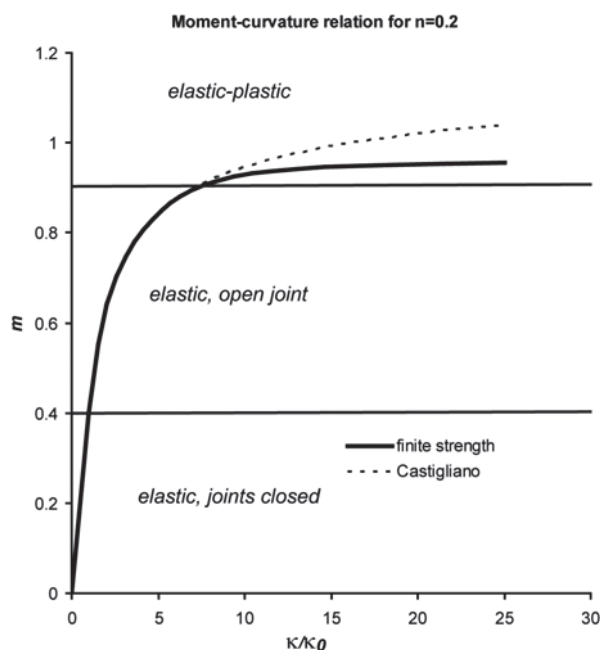

Fig. 3 Moment-curvature relation for an elastic-perfectly plastic "opening joint" model

Once part of the beam enters the elastic-plastic range, the mapping from bending moment to curvature therefore becomes almost non-unique (the slope of the curve being very small), resulting in severe problems in the context of a finite element code. In a code employing high-order trial functions, such a relation between reaction forces and deformations will automatically lead to oscillations and a premature breakdown of the algorithm, long before the actual limit load of the structure has been reached. These problems get the more severe the smaller the dimensionless normal action n is. Unfortunately, very small n is typical for most historical vaults, and even in arched masonry bridges with backfill, n rarely exceeds values around 0.25 even if we allow only $\beta = 1.0$ MN/m² for the compressive strength of the compound material mortar+stone.

This observation means nothing else that the arch offers practically no further resistance to bending once it enters the plastic range. In other words, the strains will localize, a hinge forms. In order to incorporate the finite strength model into a finite element algorithm, it is therefore advisable to replace the almost horizontal part of the moment-curvature diagram by a suitable approximation. It is obvious that the most natural approximation – a conservative one – is given by the limiting condition when the beam reaches the compressive stress at the edge (cf. Fig. 4). The gain in moment which is associated with increasing plastification is almost negligible in practical situations. Rather than implementing an elastic-plastic law like [14], we therefore opt for introducing discrete hinges at all positions where the compressive stress reaches the strength level. In contrast to our approach, the localization of strains was effectively ruled out in [30] by setting a "ductility limit", which prevents the formation of discrete hinges (associated with "ductile" rotation) and forces the arch to remain continuous.
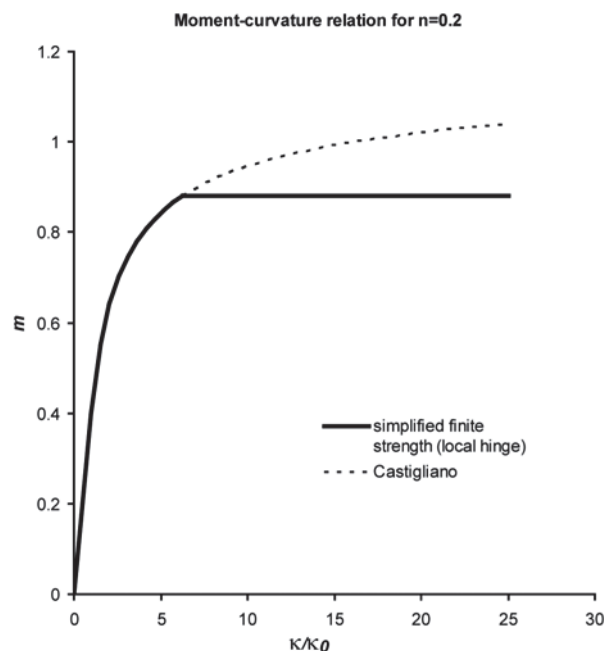

Fig. 4 Simplified moment-curvature relation for an elastic-perfectly plastic "opening joint" model

Our procedure is incorporated in an incremental loading analysis. At each load step, the program checks for all the integration points whether the compressive stress exceeds the strength β. All these integration points are marked. In an arch with infinitely thin voussoirs, the hinge would form at the point of the maximum excessive stress in each contiguous zone of open joints. In an arch with a finite number of voussoirs, the hinge will form at the joint situated next to the peak stress. Since we control the accuracy of the finite element approximation by an increase in the polynomial degree rather than mesh refinement, it is straightforward to select a mesh in which element sizes more or less reflect voussoir sizes, and to introduce the hinges at interelement boundaries. However, this is not a prerequisite and would be impractical for very small voussoirs. Nevertheless, our program always places the hinges at interelement boundaries for simplicity.

It is needless to remark that the resulting force-displacement behaviour of the arch is decidedly nonsmooth. Therefore, a classical incremental Newton-Raphson algorithm is not applicable. Rather, iterations for equilibrium are performed with a secant algorithm which always starts with the secant stiffnesses between the last equilibrated state and the origin. This means that no history information needs to be stored at element level (the whole history information being contained in the hinge locations); the additional cost caused by the linear rather than quadratic convergence of the scheme is almost negligible in practice.

3. ANALYSIS OF VARIOUS LOAD CASES

Next, we proceed by applying our incremental finite element procedure to various simple cases and compare the ultimate loads obtained to the limit loads predicted by Harvey's thrust zone method. All results shown are based on a symmetric arch with an angle of embrace of 140°, a centerline
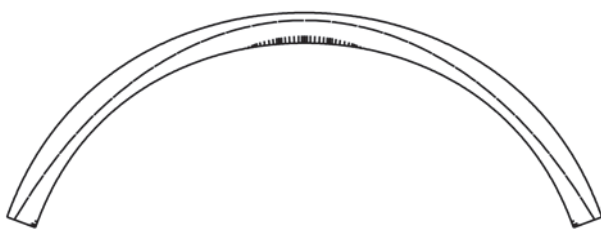

Fig. 5 The arch on rigid abutments under its own weight

Fig. 6 The arch at 1mm horizontal yield of the right abutment (scale factor 200)

Fig. 7 The arch at 2 mm horizontal yield of the right abutment (scale factor 200). Plastic hinge at apex

Fig. 8 The arch at 5 mm horizontal yield of the right abutment (scale factor 200). Three-hinge state
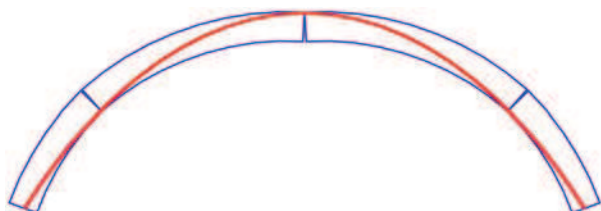

Fig. 9 "Thrust-zone" limit analysis of the arch under 200 mm abutment yield (scale factor 1)

with a radius $R = 5.0$ m, compressive strength $\beta = 1.0$ MN/m^2, arch depth $t = 0.5$ m and density $\rho = 18$ MN/m^2 of the arch material. The averaged material data for the arch (average of mortar and stone properties) were set to $E = 4000$ MN/m^2, $G = 2000$ MN/m^2. The volume fraction of the mortar joints was assumed as $\alpha = 5\%$.

Figs. 5-8 display the arch under increasing abutment yield. The "crack" marks displayed are not discrete cracks, but only symbolic indications of the joint opening at the integration points of the model. All figures show the displacements, scaled by a factor of 200, and the "line of thrust" or locus of the resultant of the compressive forces normal to the bed joints. On rigid supports, the arch shows extended zones of slightly opening joints next to the vertex and next to the springings (Fig. 5). The joints open towards the intrados at both locations. A minimal abutment movement of 1 mm towards the outside changes the picture quite strongly (Fig. 6): The joints at the top of the arch open far beyond the centerline, and two extended zones of opening joints appear on the haunches. Less than 2 mm outward movement suffice to introduce a plastic hinge at the top (Fig. 7, hinge marked by a small circle in the figure). The distance between the hinge and the extrados naturally corresponds to $h/3$. This hinge reduces the stiffness of the arch significantly. At 3.7 mm outward movement of the abutments, the next hinges form (cf. Fig. 8). These hinges appear at 35° above the horizon in our "5° voussoir" mesh. They open towards the extrados. The new hinges transform the arch into a statically determinate structure, so that our geometrically linear computation will not induce any further change of the arch state. The last figure of the series shows the arch at 5 mm outward movement of the right abutment (Fig. 8).

For an arch under dead loads, the presence of plastic hinges does not in itself constitute a risk. If the associated horizontal outward thrust H of the vault can be carried by the substructure, the arch is safe, and there is no need for an intervention, at least as long as the hinges are ductile enough to carry the required rotations.

However, if there are indications of ongoing outward movement, the arch is threatened by snap-through collapse. A very convenient way of assessing the arch on strongly spreading supports is the rigid-body model. Inspired by the works of Ochsendorf and Jagfeld, we have extended Harvey's "thrust zone method" to the case of large (geometrically non-linear) displacements (finite rigid-body rotations). Since the thrust zone method assumes a rectangular rather than wedge-shaped distribution of the compressive stresses in the plastic joint, our computations with this method have been based on the input $\beta = 1.5$ MN/m^2 in order to ensure that the hinge locations inside the joint keep the same edge distance as those produced by our continuum-mechanics based finite element analysis. The "thrust zone" approach starts from the very beginning with the assumption that the arch has already cracked and is essentially a three-hinge arch. The most unfavourable hinge positions are determined by a optimum seeking algorithm (simple hill-climbing suffices). Fig. 9 shows the state of the arch at 200 mm abutment yield, as obtained by a geometrically non-linear (large rotation) thrust-zone analysis. The crack at the apex is wide open, as well as the other two hinges on the haunches. When the arch becomes shallower as a result of the abutment spread, the thrust increases, and, as a consequence, the "thrust zone" moves towards the extrados at the springings. Once the "thrust zone" touches the extrados here,

two further hinges are generated, resulting in an unstable equilibrium state. The thrust zone analysis ignores the elastic deformation of the arch and concentrates all the "opening joint" behaviour at discrete hinges. However, once the arch has reached the three-hinged state, the rigid-body movements of the three-hinge system dominate. This can be clearly seen from a comparison of the "cracking continuum" vs. "thrust zone" computations (Fig. 10).
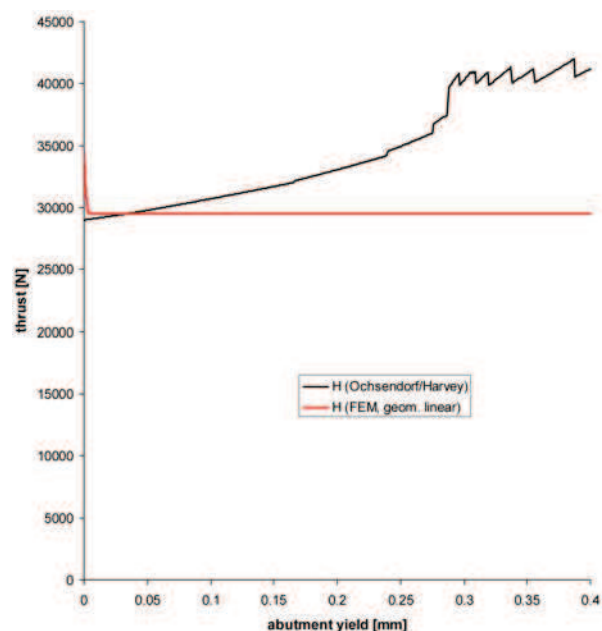

Fig. 10 Comparison of geometrically linear finite element analysis and geometrically linear limit analysis using the thrust zone concept

The FEM curve (Fig. 10, in red) is able to represent the sharp drop of the arch thrust at small displacements, but – due to our geometrically linear code – it does not represent the increase of the thrust which is caused by the flattening of the arch at large abutment yields. Conversely, the thrust zone method assumes that the arch is already in three-hinged state from the very beginning, which is not true. Therefore, it yields a lower bound on the horizontal thrust at small displacements. The two curves intersect at roughly 3.5 mm outward movement. In fact, geometric nonlinearity is not yet important at such small displacements, but is the dominating factor at larger abutment yields, as evidenced in the figure; at larger displacements, the thrust zone method represents the actual arch behaviour correctly (the three-hinge system). Therefore, the two methods complement each other almost perfectly. With increasing abutment yield, the plastic hinges gradually jump from their starting positions at 35° degree above the horizon to 60°. The jumps are clearly visible in the curve. Finally, the thrust zone touches the contour of the arch not only at the three hinges, but also at the springings (outward movement of 305 mm). This introduces a sharp increase in the computational thrust; however, the computation can be continued for even larger outward movements (up to 533 mm). The solutions (hinge locations) corresponding to this part of the thrust-deflection curve are very unstable (as evidenced by the zigzagging curve), and in reality, this last part of the curve cannot be obtained because the arch is evidently in an instable five-hinge mechanism state. For the arch considered, the 305 mm displacement is the practical limiting value. In real-life situations, the actual

abutment spread can often be measured, assuming that the supporting walls were originally vertical, so that the thrust zone method provides valuable information on the safety of the arch in the sense of answers to the question "how much can the abutment spread increase beyond its current value without entailing collapse".

Next, we study the arch under the action of a concentrated load with our finite element procedure. We place a constant load on the section of the arch contained between the 50° and 60° angles above the horizon. Then, we increase this load. In the following figures, the load is represented as an equivalent "pile of material" on top of the arch (the pile material corresponding to the arch material). At approximately 2 m of additional load, the first hinge forms at the extrados of the abutment opposite the load (Fig. 11).
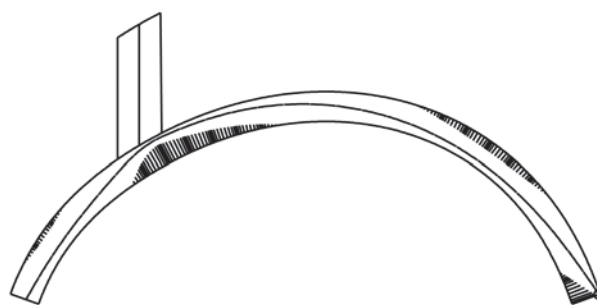

Fig. 11 Arch under the action of an additional load. Formation of the first hinge (scale factor 200)
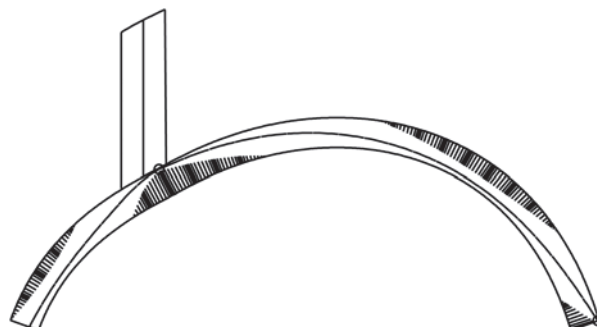

Fig. 12 Arch under the action of an additional load. Formation of the second hinge (scale factor 200)

Further increase of the load leads to the formation of more hinges. At approximately 2.6 m of additional load, a second hinge appears at the inner end of the loaded zone (Fig. 12). Increasing the load to approximately 3.3 m yields a third hinge, this time close to the abutment beneath the load (Fig. 13). Finally, a fourth hinge forms at the ultimate load of 3.37 m and transforms the arch into a four-bar mechanism (Fig. 14). For comparison, we show the same arch also in the "thrust zone" analysis, at a load of 3.4 m (Fig. 15). It is evident that the thrust zone analysis is able to predict a very reasonable estimate of the actual collapse load. At 3.4 m load, the thrust zone analysis renders hinge positions at 29°, 60° and 122.5°, which agree very well with the hinge positions as obtained by the finite element method. Furthermore, the thrust zone just touches the extrados at thge right abutment with a load of 3.4, indicating the formation of the final hinge. Even though the sequence of hinge formation is unknown, the actual limit load is correctly predicted, and the correct hinge arrangement is found.
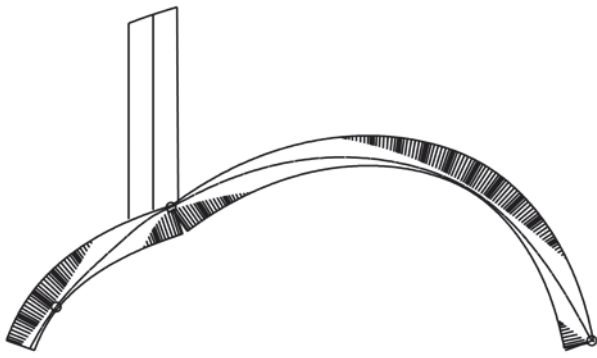
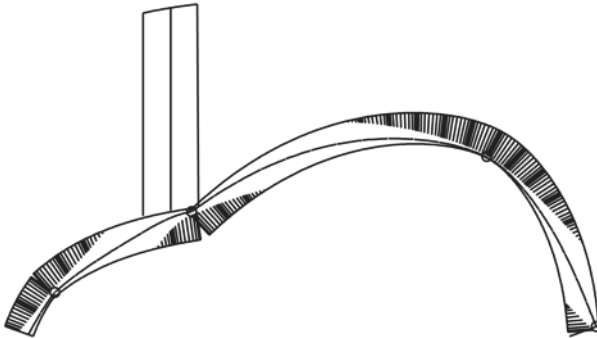Fig. 13 Arch under the action of an additional load. Formation of the third hinge (scale factor 200)

Fig. 14 Arch under the action of an additional load. Formation of the fourth hinge (scale factor 200)
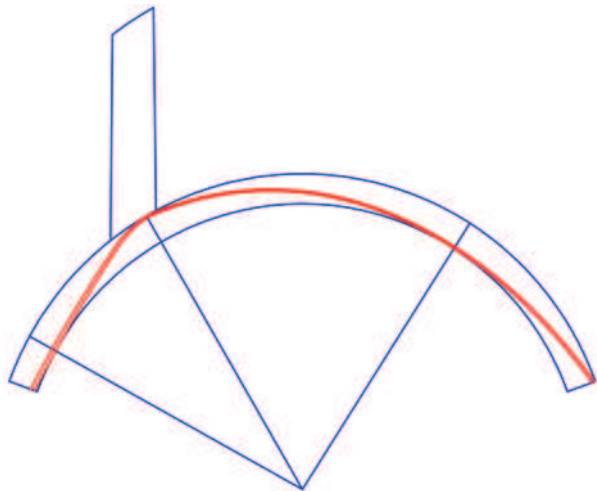

Fig. 15 Thrust zone analysis of the arch with additional load. Limit load and mechanism agree very well with the finite element prediction
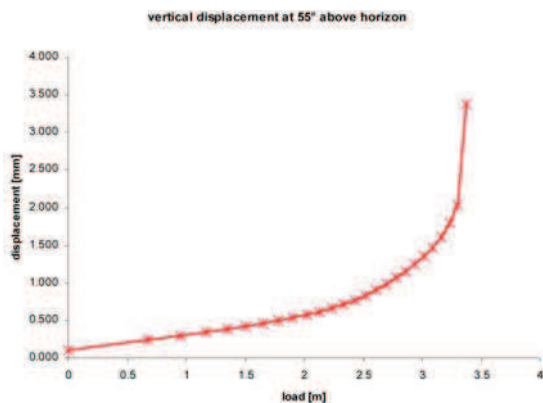

Fig. 16 Load-displacement function of the arch with additional load. The recorded displacement is the vertical displacement of the point under the center of the loaded area (55° angle above the horizon)

Finally, Fig. 16 shows the development of the vertical settlement of the arch under the load, as the load is progressively increased until collapse (results of finite element simulation). Each hinge leads to a kink in the curve, whereas the spreading of the regions with elastic opening joints induces a gradual softening of the arch. It is evident that particularly the last part of the computation is markedly non-linear, requiring relatively small load steps for accuracy. In our example, the load was applied in 25 progressively decreasing steps (square root progression).

Naturally, our finite element approach can be easily extended to handle not just a single arch, but also complex systems of arches and piers, such as multi-span bridges. Fig. 17 shows such an example. The "tas-de-charge" blocks have been modelled by purely elastic beam elements, while all the other members of the structure are allowed to crack – and finally form a hinge – under the load. Of course, our simple analysis based on beam elements is restricted to cases where the assumption is valid that the cracks will follow a single joint through the thickness of the member, rather than cracking in a zig-zag (or stepwise) pattern. A thick arch consisting of several (interlocked or non-interlocked) rings of voussoirs or a thick pier consisting of several blocks in thickness do not fulfil these restrictions.

4. THE BARREL VAULT WITH LUNETTES AND THE CROSS VAULT

The good agreement between the limit analysis estimate and the incremental finite element/discrete hinge procedures gives rise to the hope that many real-life vaults can be rapidly assessed via the geometrically non-linear thrust zone method. However, whereas the mechanisms associated with arches or plane arrangements of several arches and piers (multispan bridges) are comparatively simple, it is not so clear which mechanisms are effective in real three-dimensional vaults. Anyway, a situation which is frequently encountered in the nave of historic churches and other vaulted buildings is an arrangement of several cross-vaults balancing each other in longitudinal direction. Furthermore, many historical nave vaults have the form of a barrel vault with lunettes. Visually, a series of cross vaults and a barrel vault with lunettes are often virtually undistinguishable in the view from below. Only in the aspect from above, the true structure of the vault becomes evident. Many gothic vaults with a dense network of ribs are in fact barrel vaults with lunettes.

In order to get a simplified approach to the safety assessment of such vaults, we have to assume a failure mechanism. For the most important case of yielding abutments, the following mechanisms offer themselves for consideration:
– The lunettes separate from the main barrel at the groins. Essentially, the lunettes stand unchanged when the abutments yield and the main barrel rotates inwards. This kind of mechanism can be triggered by ill bond at the groins (a natural effect of barrel vault masonry constituted by courses of bricks running parallel to the axis of the barrel) and by high back-fill.
– The lunettes stick to the main barrel and are essentially lifted up from their bases; they rotate inward together with the barrel when the abutments yield. This behaviour is unlikely in typical barrel/cross vaults whith straight courses of masonry running parallel to the barrel/lunette
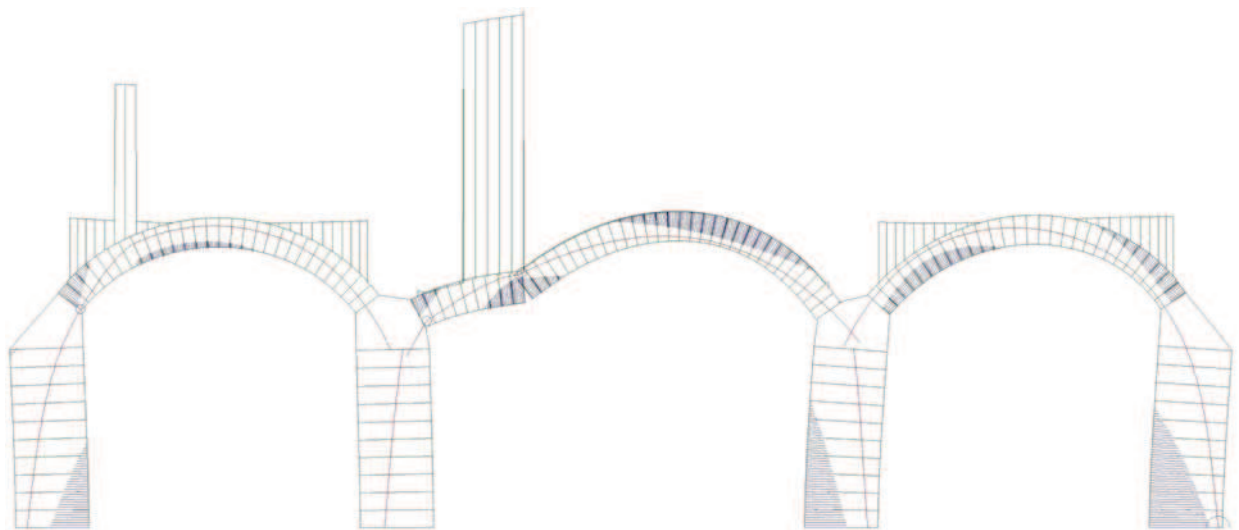
Fig. 17 A system of arches and piers subjected to local loads. Near-collapse state. Circle marks indicate fully established hinges, whereas hashed areas are "cracked" (opening joints), but still below the compressive limit stress

axis. However, it is a limit case for any mechanism which involves cracking of the lunette. It also describes a limit case for any lunettes which are not bonded with the longitudinal walls of the building (lunette separating from the wall). In some real-life cases, horizontal cracks at the bases of the lunettes are, nevertheless, observable.

– The lunette cracks according to the well-known "Sabouret" mechanism. In this case, the upper part of the lunette remains fixed to the main barrel, whereas the outer part does not take part in the rotation.

All these three mechanisms are essentially plane mechanisms. The thrust zone allows us to account approximately for the fact that the stress is concentrated in the lower parts of the vaults towards the tas-de-charge. The assumptions about the mechanism can be easily verified by recording the location and orientation of the actual cracks in the vault.

Let us demonstrate the concept with an example. Assume that we have a main barrel of 5 m radius with 25 cm thickness and an angle of embrace of 120° (i.e., abutments at 30° above the horizon). We consider a portion of this barrel vault which is 11 m long. The density of the vault material is the same as before. This longitudinal vault is intersected by lunettes with 4.5 m radius, 25 cm thickness. The lunettes are assumed to start at the same height as the main vault, and they have a horizontal ridge. The nave is assumed to be 10 m wide. Since the radius of the lunettes is less than the radius of the main barrel, they do not reach up to the ridge of the main barrel. The scheme corresponds to a widespread model of 16th and 18th century vaults. If we assume a periodic arrangements of such vault bays, it suffices to analyze one half of the vault. We assume a compressive strength of $\beta = 1.0$ MN/m² as before, and rigid supports.

If we ignore the lunettes altogether, the barrel vault exerts a horizontal thrust of approximately 185 kN on its supports (Fig. 18; the weight of the pure barrel vault is 518 kN). The cracks (hinge lines) are at the crown of the vault and at 43.5° above the horizon. Next, we introduce the lunettes. If we assume that the lunettes will crack vertically (Sabouret cracks, cf. Fig. 19), then the hinge lines in the main barrel appear at 42° above the horizon, and the thrust of the bay increases to 187 kN. Conversely, if we assume that the lunettes separate

completely from the main barrel and do not partake in its rotation, then the lower limit of the thrust given by the thrust zone model is 184 kN, with hinges at 47° above the horizon. Finally, the assumption of lunettes sticking to the main barrel and rotating with it, lifting off the lowest part, yields a limit analysis thrust of 177 kN, and hinge lines at 34.5° above the horizon (Fig. 20). Evidently, the Sabouret case is the most un-
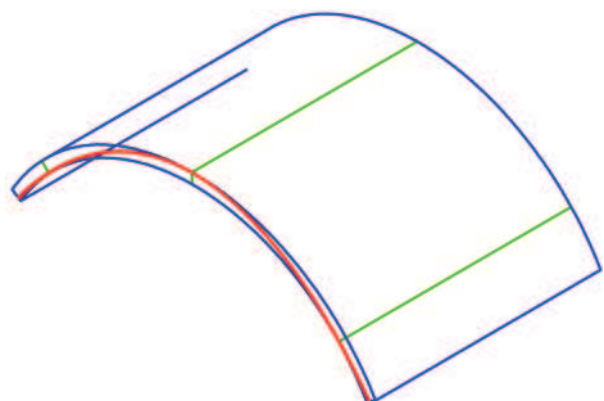

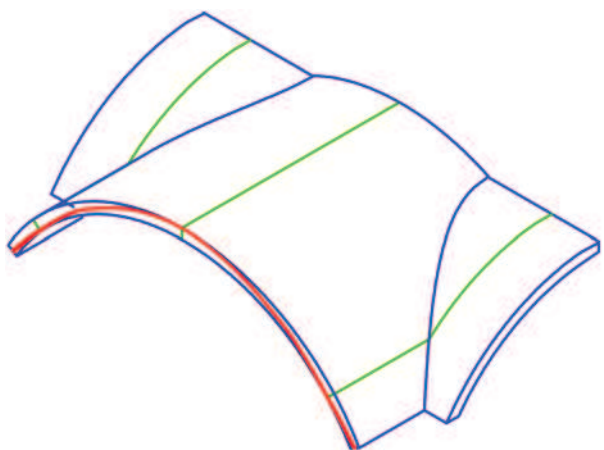Fig. 18 Barrel vault with lunettes ignored. Green lines indicate hinge lines

Fig. 19 Barrel vaults with lunettes. Limit analysis result with thrust-zone technique, assuming a rigid-body mechanism in accordance with the formation of Sabouret cracks. Green lines indicate hinges or cracks
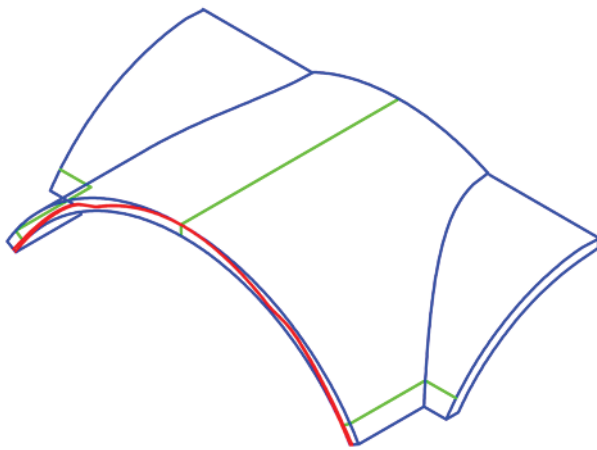
Fig. 20 Barrel vault with lunettes. Results obtained with the assumption that the upper part of the lunette sticks to the main barrel and rotates with it, lifting off the lower part
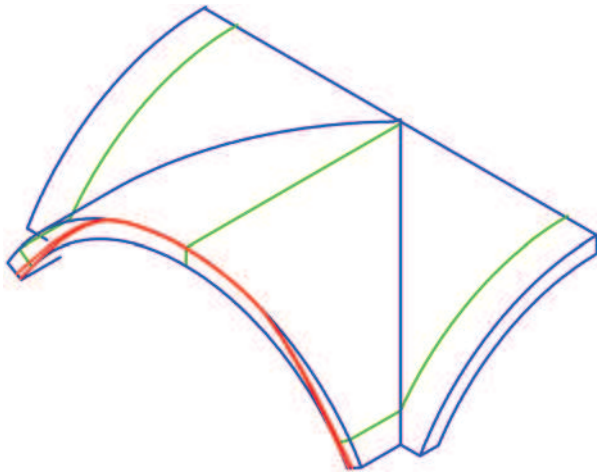

Fig. 21 The cross vault with Sabouret cracks

favourable one. Playing with the three distinct failure modes, it is always straightforward and easy to determine the most unfavourable one. In most practical cases, the limit mecha-

nism is almost identical to the case of a barrel vault without any lunettes at all, because the hinge lines are typically so high above the springings that only a small portion of the lunettes actually takes part in the mechanism. Therefore, a very quick assessment may even be done on the basis of a very simple plane computation (arch model), verifying ex post whether the portion of the lunettes taking part in the mechanism was indeed negligible or not.

If we increase the radius of the lunette to 5 m, our barrel vault is transformed into a cross vault with horizontal ridges. In this case, a vault thickness of 25 cm turns out to be insufficient with $\beta = 1.0$ MN/m^2. If we increase the thickness to 40 cm, the vault is stable again. However, the differences between the three assumed mechanisms get greater the more the vault resembles a cross vault. In the cross vault and similar geometries, the Sabouret mechanism is always the most unfavourable one. In our example (Fig. 21), it renders 285 kN of thrust for the whole bay.

5. CONCLUSIONS

Discrete hinges forming in arches and vaults are essential for the realistic assessment of their structural safety. Purely continuum-mechanics based methods are well suited for the simulation of the load-deflection behaviour of vaulted masonry structures under service loads, but are ill suited for the analysis of the collapse state. Limit analysis method provide sharp estimates of the load carrying capacities since the elastic (both linear-elastic and elastic-open-joint) contribution to the limit loads is typically negligibly small. Distinct element methods, while in theory well suited to vault analysis, are too complicated to use in practice. Therefore, it is reasonable to bridge the gap between continuum-mechanics based approaches and classical limit analysis by introduction of suitable localized strains (hinges). Limit analysis methods are easily to extend to both geometrically non-linear (large abutment spread) situations and also to some practically relevant three-dimensional situations which essentially reduce to plane hinge mechanisms. This makes them very attractive for practical assessment purposes.

REFERENCES

[1] Castigliano A.P. (1879) *Théorie de l'équilibre des systèmes élastiques.* Turin: Negro, and Paris: Baudry.

[2] Wu L., Hughes T. (2010) Castigliano based analysis of single span masonry arch bridges using a spreadsheet. In: *Proc. 6th Int. Conf. Arch Bridges Arch '10*, Fouzhou, 506-513.

[3] Sinopoli A., Foce F. (2001) Theoretical research on masonry and masonry arches in Italy. In: *Arch '01 – Third international arch bridges conference.* Paris, 323-342.

[4] Lucchesi M., Padovani C., Pasquinelli G., Zani N. (1997) On the collapse of masonry arches. In: *Meccanica*, 32, 327-346.

[5] Loo Y.-C., Yang Y. (1991) Cracking and failure analysis of masonry arch bridges. In: *ASCE Journal of Structural Engineering*, 117, 1641-1659.

[6] Barthel R. (1991) *Tragverhalten gemauerter Kreuzgewölbe*. Ph.D. thesis Univ. Karlsruhe (TH)

[7] Trautz M. (1998) *Zur Entwicklung von Form und Struktur historischer Gewölbe aus der Sicht der Statik*. Ph.D. thesis Univ. Stuttgart.

[8] Krausz K. (2002) *Tragverhalten gemauerter Tonnengewölbe mit Stichkappen*. Ph.D. thesis Univ. Stuttgart.

[9] Lourenço P. (1996) *Computational strategies for masonry structures*. Ph.D. thesis TU Delft.

[10] Jagfeld M. (2000) *Tragverhalten und statische Berechnung gemauerter Gewölbe bei großen Auflagerverschiebungen – Untersuchungen mit der Finite-Elemente-Methode*. Ph.D. thesis TU München.

[11] Schlegel R. (2004) *Numerische Berechnung von Mauerwerkstrukturen in homogenen und diskreten Modellierungsstrategien*. Ph.D. thesis Univ. Weimar.

[12] Lourenço P. (2001) Analysis of historical constructions: From thrust-lines to advanced simulations. In: *Historical Constructions*, 91-116.

[13] Betti M., Drosopoulos G.A., Stavroulakis G.E. (2007) On the collapse analysis of single span masonry/stone arch bridges with fill interaction. In: *Proc. 5th Int. Conf. Arch Bridges Arch '07*, Funchal, 617-624.

[14] Crisfield M.A. (1985) *Finite element and mechanism methods for the analysis of masonry and brickwork arches*. Transport and Road Research Laboratory, Research Report 19. Crowthorne: Highways and Structures Department.

[15] Aita D., Barsotti R., Bennati S. (2011) Equilibrium of pointed, circular and elliptical arches bearing vertical walls. In: *ASCE Journal of Structural Engineering* (preview document published 18. 10. 2011).

[16] Molins C., Roca P. (1998) Capacity of masonry arches and spatial frames. In: *ASCE Journal of Structural Engineering*, 124, 653-663.

[17] Heyman J. (1966) The stone skeleton. In: *International Journal of Solids and Structures*, 2, 249-279.

[18] Taylor N., Mallinder P. (1993) The brittle hinge in masonry arch mechanisms. In: *The Structural Engineer*, 71, 359-366.

[19] Brencich A., Morbiducci R. (2007) Masonry arches: historical rules and modern mechanics. In: *International Journal of Architectural Heritage*, 1, 165-189.

[20] Smith F.W., Harvey W.J., Vardy, A.E. (1990) Three-hinge analysis of masonry arches. In: *The Structural Engineer*, 68, 203-213.

[21] Ochsendorf J.A. (2006) The masonry arch on spreading supports. In: *The Structural Engineer*, 29-35.

[22] Livesley R.K.(1978) Limit analysis of structures formed from rigid blocks. In: *International Journal for Numerical Methods in Engineering*, 12, 1853-1871 Gilbert 2007.

[23] Gilbert M., Melbourne C. (1994) Rigid-block analysis of masonry structures. In: *The Structural Engineer*, 72, 356-361.

[24] Bićanić N., Stirling C., Pearce C.J. (2003) Discontinuous modelling of masonry bridges. In: *Computational Mechanics*, 31, 60-68.

[25] Gilbert M. (2007) Limit analysis applied to masonry arch bridges: state-of-the-art and recent developments. In: *Proc. 5th International Conference on Arch Bridges Arch '07*, Funchal, 13–28.

[26] Lemos J. (2007) Discrete element modeling of masonry structures. In: *International Journal of Architectural Heritage*, 1, 190-213.

[27] Casapulla C., D'Ayala D. (2001) Lower bound approach to the limit analysis of 3D vaulted block masonry structures. In: *Computer methods in Structural Masonry*. Swansea: Computer and Geotechnics Ltd.

[28] D'Ayala D., Casapulla C. (2001) Limit state analysis of hemispherical domes with finite friction. In: *Historical Constructions, Possibilities of Numerical and Experimental Techniques*.

[29] D'Ayala D. Tomasoni E. (2011) Three-dimensional analysis of masonry vaults using limit state analysis with finite friction. In: *International Journal of Architectural Heritage*, 5, 140-171.

[30] Brencich A., De Francesco U. (2004) Assessment of multispan masonry arch bridges I: Simplified approach. In: *ASCE Journal of Bridge Engineering*, 582–590.

[31] Szabó B., Babuska I. (1991) *Finite Element Analysis.* New York: Wiley.

Abstract

The present contribution discusses various approaches towards the numerical analysis of arches, particularly finite element methods based on a continuum mechanics approach vs. rigid-body approaches. We employ beam elements and a simple model for the interaction between axial compression and bending. The model is based on the assumption that cracks follow the radial joints, and on a simplified concept of incorporating finite compressive strength. We establish a transition from finite element methods to rigid body methods by the introduction of discrete hinges in the course of an incremental finite element analysis. We show that rigid body methods based on the "thrust zone" approach developed by Harvey et al. (1990) render sharp estimates of the ultimate loads, and that the "thust zone" concept provides valuable estimates for large displacements. Finally, we extend the rigid-body approach to the case of barrel vaults with lunettes.